Carbon Nanostructure Examined by Lattice Fringe Analysis of High Resolution Transmission Electron Microscopy Images

Randy L. Vander Wal[1], Aaron J. Tomasek[1], Ken Street[2] and William K. Thompson[2]

[1] *National Center for Microgravity Research c/o NASA Glenn Research Center MS 110-3, 21000 Brookpark Road Cleveland, Ohio 44135*

[2] *NASA Glenn Research Center 21000 Brookpark Road Cleveland, Ohio 44135*

Corresponding author e-mail address: aaron.j.tomasek@grc.nasa.gov

Introduction

Although soot represents one of the very first nanostructured materials, it has rarely been considered as such. For decades, combustion research has focused on its formation and growth, in lieu of particle interior structure. However, carbon soot nanostructure has been shown to change dramatically based upon factors such as fuel source and temperature [1]. Layer planes with larger in-plane dimensions characterize graphitic carbons, while amorphous carbons contain shorter, disjointed segments [2]. By virtue of geometry, larger layer planes contain fewer carbon atoms at edge sites relative to basal plane sites. The connection between layer plane dimensions and reactivity towards oxidation is due to the anisotropic reactivity of the graphitic segments comprising the carbon. Carbon atoms within basal plane sites, surrounded by other carbon atoms, exhibit a far lower reactivity towards oxidation than those located at the periphery of such segments (so-called edge sites) [3-7].

Changes in the carbon nanostructure, such as an increase in graphitic layer plane length, have been correlated with reactivity loss [8-9]. Layer plane extension arises from a reorientation/reorganization of material. Layer plane segments can grow by bonding to adjacent graphene segments and by addition of amorphous carbon material within the soot particle [10-13]. High-resolution transmission electron microscopy (HRTEM) can reveal the graphitic structure of carbon, i.e. its nanostructure. These images can provide a direct measure of the length, shape and orientation of the graphitic fringes at any particular depth in the materials, as determined by the focal plane [14]. As a measure of molecular order, quantification of the graphene segment dimensions could potentially be used to assess the reactivity of carbon towards oxidation. Towards this goal this work sought to develop such an algorithm for soot. Lattice fringe analysis has been employed to explain reactivity issues of other types of carbons, including solid fuel chars [15-16].

Experimental

Samples of carbon black (Cabot R250 from Cabot Corporation) were heat-treated in a

LECO EF-400 resistance heated furnace using a graphite crucible under a He atmosphere for 30 minutes. The furnace was operated in power mode to maintain temperature stability and reproducibility. TEM images were taken using a Phillips CM200 with Gatan image filter (GIF) for digital imaging with live Fourier transforms having nominal resolution of 0.14 nm. The instrument operated at 200 keV using a LaB_6 filament. Gatan image software, v.3.4 was used for microscope operation. A Renishaw Model 2000 Raman Microscope that uses a 25 mW Ar^+ ion laser operating at 514.5 nm was used to collect Raman spectra. The spectra presented here are single scans and are corrected for background. Spectra were taken from at least three areas of each sample to ensure that the spectra are representative of the material.

Using a fringe analysis program, the distribution of fringe lengths can be obtained. The algorithm exists as a macro, running under Optimas version 6.5 [17]. Clearly any image analysis program needs input parameters to deal with the limitations in distinguishing fine features, gray-scale levels and overall image contrast as determined by focusing variability. Therefore, this program features a menu driven interface for selection of the region of interest, correction for uneven illumination across the image (common in HRTEM imaging), spatial filtering prior to processing and a binary thresholding operation which extracts fringe areas from the background. The program also allows retouching to blank out any artifacts that lie within the region of interest that do not correspond to image data. Execution of the macro utilizes these parameters to convert an image from grey-scale to binary. Carbon layer plane thickness, which may increase with decreasing focus quality, is made constant at one pixel, creating a skeletonized, binary image. Non-physical conditions, such as sharp bends are also detected and separated. Among other outputs, the program displays the length of each fringe. A histogram is readily created from such data.

Results and Discussion

Figure 1 shows HRTEM images of the carbon subjected to different heat treatment temperatures of 1350, 1950, 2300 and 3000°C, each representative of over fifty images. The growth of graphitic structure becomes apparent with increasing thermal treatment. As observed for thermally annealed carbon blacks, the particles evolve towards faceted polygons with hollow interiors [18]. The net effect of increasing heat treatment temperature is to induce an increase in the number of stacked graphitic segments, improve their relative alignment and in particular, extend their length.

As observed in Figure 2, the skeletonized images display high similarity to the length and orientation of lattice fringes seen in the HRTEM input images. These binary images show a clear increase in fringe length across the series of annealed carbon blacks. Individual fringe lengths were extracted from these images and the subsequent distributions are summarized in the histograms presented in Fig. 3. With increasing heat treatment temperature, the relative percentage of short fringes declines while that of longer fringes increases. This increase is attributed to both joining of adjacent fringes, where their mobility is aided by the elevated temperature, and addition of adjacent random and disordered carbon to lamella.

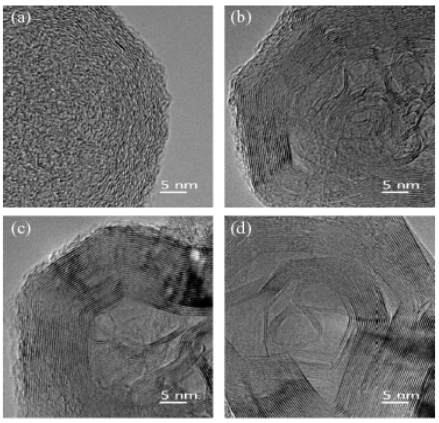

Figure 1. HRTEM images of the carbon black prepared by heat treatment at temperatures of a) 1350, b) 1950, c) 2300 and d) 3000°C.

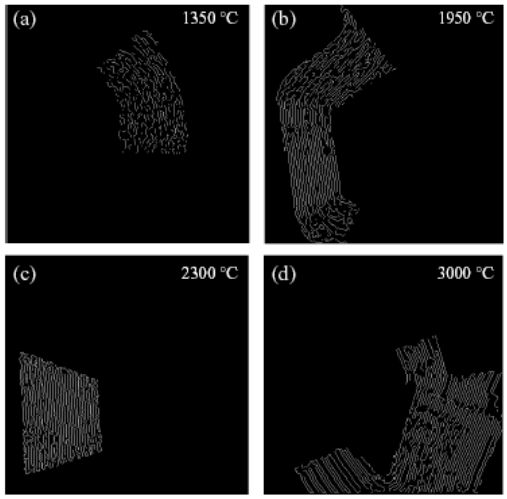

Figure 2. Skeletonized images obtained by applying the lattice fringe analysis program to the HRTEM images shown in Fig. 1.

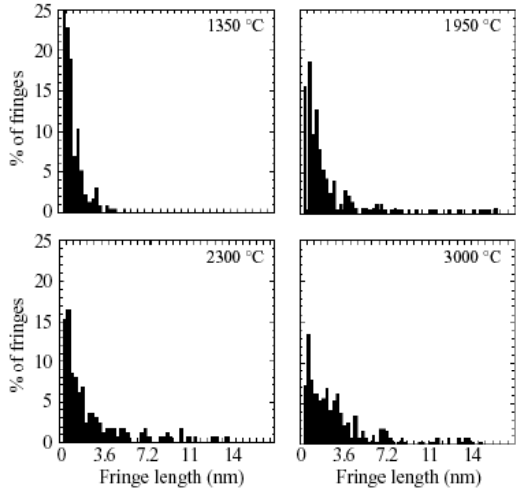

Figure 3. Histograms of the fringe lengths from the binary images shown in Fig. 2.

Image fringe analysis provides a non-integrated, direct measure of the soot nanostructure, which unlike traditional methods, allows for a detailed analysis of carbon nanostructure properties, including fringe length and curvature using nanogram-quantities of material. Nevertheless, it is instructive to compare the fringe analysis results with those provided by Raman for comparison of the fringe length data, i.e. relative graphitic content.

Raman spectroscopy has been tested as a method for determining the planar crystallite dimensions of carbons that possess limited long-range order [19-20]. Two spectral peaks characterize the first order Raman spectra of carbon materials; a very strong, high-frequency, in plane stretching mode (E_{2g} or "G" peak near 1580 cm^{-1}) and a weaker, low-frequency mode (A_{1g} or "D" peak near 1360 cm^{-1}) [21]. The intensity ratio of these peaks has been interpreted as a measure of the in-plane crystallite dimensions [19]. Strong monotonic correlations have been shown between the D/G intensity ratio and heat treatment temperature [22-23].

The Raman spectra of the different heat-treated carbon black samples are plotted in Fig. 4. The change in relative intensities is consistent with increasing graphitization induced by higher temperatures. The narrowing of the D and G peaks indicates increasing homogeneity of the sample as disordered carbon is reorganized and/or joins to growing lamella. Figure 5 shows graphs of the integrated intensity ratio of the G and D peaks of the carbon nano-onions as a function of the heat treatment temperature. Plotted for comparison are the medians of the fringe length histograms shown in Fig. 4 corresponding to the selected heat treatment temperatures.

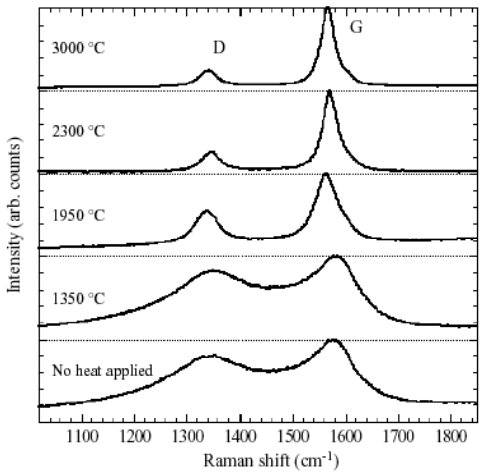

Figure 4. Raman intensity plots (1st order spectra) for the heat-treated carbon black.

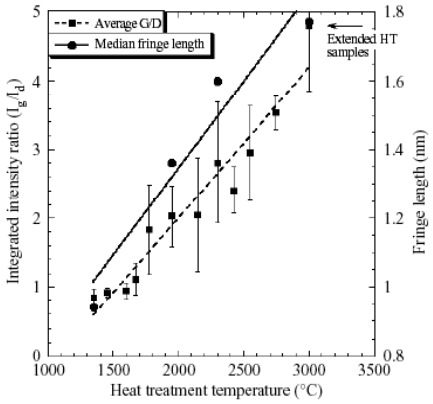

Figure 5: Plots of the mean lattice fringe lengths obtained from histograms in Fig. 3 and Raman (I_G/I_D) peak ratios obtained from Fig. 4.

Conclusions

A lattice fringe analysis program has been developed to quantify the data conveyed by HRTEM images. By providing a direct measure of the molecular level of graphitic structure, it is expected that its application could provide predictive capabilities for carbon reactivity, particularly towards oxidation. The robustness of this program is demonstrated by using a series of carbon blacks possessing different levels of graphitic structure. Its credibility is benchmarked against a traditional measure of graphitic structure, as provided by Raman analysis.

Acknowledgments

This work was supported by a NASA NRA 99-HEDs-01 combustion award (RVW) administered through NASA cooperative agreement NCC3-975 with The National Center for Microgravity Research on Fluids and Combustion (NCMR) at The NASA Glenn Research Center. The authors gratefully acknowledge Gordon M. Berger, Michael Pamphlet, Christina Taylor and Patrick Rodgers for assistance with the experiments and Dr. Y. L. Chen and David R. Hull for the TEM imaging.

Disclaimer

Trade names or manufacturers' names are used for identification only. This usage does not constitute an official endorsement, either expressed or implied by either the National Aeronautics and Space Administration or The National Center for Microgravity

References

1. Vander Wal, R. L., and Tomasek, A. J., *Combustion and Flame*, **2004**, 136, 129, and references therein.
2. Wilks, K. R., Mastalerz, M., Bustin, R. M. and Ross, J. V., *Int. J. of Coal Geology* **1993**, 22, 247.
3. Smith, W. R. and Polley, M. H., *J. Chem. Phys.* **1956**, p. 689.
4. Thomas, J. M., Microscopy studies of graphite oxidation, in The Chemistry and

Physics of Carbon, (P. L. Walker, Jr., Ed.) **1965**, Vol. 1, Chp. 2.
5. Henning, G. R., Chemistry and Physics of Carbon, (P. L. Walker, Jr., Ed.), **1966**, Vol. 2, Chp. 1
6. Levy, M., and Wong, P., *J. of The Electrochem. Soc.* **1964**, 11, 1088.
7. Rosner, D. E. and Allendorf, H. D., *AIAA Journal* **1968**, 6, 650.
8. Donnet, J. B., *Carbon* **1982**, 20, 267.
9. Marsh, H., Introduction to Carbon Science, Butterworths, London, **1989**, Chp. 4, pp. 107.
10. Heckman, F. A. and Harling, D. F., *Rubber Chem. And Technol.* **1966**, 39, 1. See also The Presentation at the Annual meeting of the Division of Rubber Chemistry, The American Chem. Soc., Miami Beach.
11. Hess, W. M., Ban, L. L., Eckert, F. J. and Chirico, V. *Rubber Chem. and Technol.* **1968**, 41, 356.
12. Marsh, P. A., Voet, A., Mullens, T. J. and Price, L. D., *Rubber Chem. and Technol.* **1970**, 43, 470.
13. Vander Wal, R. L., and Choi, M. Y., *Carbon* **1999**, 37, 231.
14. Vander Wal, R. L., *Combust. Sci. and Technol.* **1997**, 126, 333.
15. Shim, H.-S., Hurt, R. H. and Yang, N. Y. C., *Carbon* **2000**, 38, 29.
16. Dukhan, X. Z., Kantorovich, I. I., Bar-Ziv, E., Kandas, A., and Sarofim, A. F., Twenty-Sixth Symposium (International) on Combustion, The Combustion Institute, Pittsburgh, PA **1996**, pp. 3111-3118.
17. Optimas, Media Cybernetics L.P., Siver Springs, MD.
18. Millward, G. R., and Jefferson, D. A., Lattice resolution of carbons by electron microscopy, in "The Chemistry and Physics of Carbon", Vol. 14, (P. L. Walker and P. A. Thrower, Eds.), Marcel Dekker Inc., New York, **1970**, Chp. 1.
19. Knight, D. S., and White, W. B., *J. Mater. Sci.* **1989**, 4, 385.
20. Fischbach, D. B., and Couzi, M., *Carbon* **1986**, 24, 365. (and references therein).
21. Tuinstra, E., and Koenig, J., *J. Chem. Phys.* **1970**, 53, 1126.
22. Nakamizo, M., Kammereck, R., and Walker, Jr., P. L., *Carbon* **1974**, 12, 259.
23. Emmerich, F. G., *Carbon* **1995**, 33, 1709.